ANALYSIS OF THE INFLUENCE OF ADDITIONAL UNSPRUNG MASS OF IN-WHEEL MOTORS ON THE COMFORT AND SAFETY OF A PASSENGER CAR

GRZEGORZ ŚLASKI[1], ADAM GUDRA[2], ADAM BOROWICZ[2]

Poznan University of Technology, RRM Technic

Summary

Results of simulation research and of some experimental tests on the influence of additional unsprung mass of in-wheel motors on the comfort and safety of a passenger car have been presented. This research had its origins in research and development works aimed at developing an additional electric powertrain for any front-wheel-drive passenger car with an IC engine, undertaken to convert such a vehicle into one with two alternative driving systems powered by engine fuel and electric energy for the car usability to be enhanced and for the car operation costs to be lowered. An idea was adopted to install two electric motors in hubs of the wheels that are not driven in the original vehicle version (rear wheels in this case). Based on analyses of similar engineering solutions and on design assumptions made by the authors, the motor mass was estimated and added to the unsprung mass in the form of extra weights fixed to the stub axle, with modifying accordingly the mass values adopted in the mathematical quarter-car suspension model that was used for the computer simulations. Results of the experimental tests were analysed with taking into account an analysis of the RMS car body acceleration value vs. frequency curves; to examine the simulation test results, the frequency response functions were calculated and analysed for sprung mass accelerations and dynamic wheel loads and the EUSAMA indicator values (normally used at shock absorber testing) were determined.

Keywords: wheel motors, unsprung mass, safety

1. Introduction. In-wheel electric motors

The history of works on using electric drive systems in vehicles began even before the idea arose to use combustion engines for this purpose. The period where such systems took a significant share among various powertrain types occurred as early as at the beginning of the development of motor vehicles, i.e. in the first decade of the 20th century. In 1900, 35% of the 4 200 motor cars sold were electrically driven and another 40% of the total

[1] Poznan University of Technology, Institute of Machines and Motor Vehicles, ul. Piotrowo 3, 60 965 Poznań, Poland, e mail: grzegorz@slaski.eu, tel. 61 665 22 22

[2] RRM Technic Sp. z o.o., ul. Gdyńska 131, 62 004 Czerwonak, Poland, e-mail: info@rrm-technic.pl, tel. 61 851 07 10

consisted of vehicles powered by steam, as against a mere 22% taken by cars with internal combustion (IC) engines [4].

The variety of concepts regarding the location of electric motors in cars included an idea to incorporate such motors into wheel hubs so that the motors could directly drive the vehicle wheels. It was as long ago as in 1884 when W. Adams [1] patented a motor to be placed in the hub of a wheel intended for a light rail vehicle. In 1898, Ferdinand Porsche built a prototype of an electric vehicle with in-wheel motors; at first, the motors drove wheels of one axle and afterwards, two axles were also driven (about 300 such vehicles were sold) [7].

At present, this concept is being developed by many companies. Some of the designs, such as Protean Electric Ltd. [8] or Hyundai Mobis [2], barely consist of a motor integrated with a wheel hub; other manufacturers, such as Michelin [5], Bridgestone, or Siemens [6], propose also solutions that include a complete electric powertrain and springing system with electric motors being placed in vehicle wheels.

In the concept developed by RRM Technic, in which the research work described herein had its origins, electric motors are installed in rear vehicle wheels in such a way that the braking system and wheel suspension system components remained unchanged. This required a motor to be developed that would be fixed to the wheel hub and would have an external rotor and a stator whose windings would be deployed on a circle with its diameter exceeding that of the brake mechanism. The motor will have no conventional shaft and its rotor will be supported by vehicle wheel bearings. The rotor with permanent magnets will be installed on wheel studs between the brake disc and the wheel disc.

Batteries and control system components will be placed in the spare tyre well. The vehicle will be provided with an on-board battery charger, which will make it possible to charge the battery from a standard 220 V outlet socket. For the vehicle to function correctly in the pure electric drive mode, the IC engine auxiliaries will also have to be modified. In particular, such vehicle components as mechanical power steering pump, air conditioning compressor, heating system, or brake vacuum pump, will be driven by electric motors.

Fig. 1. A concept of the in-wheel electric motor

2. Methods of examining the influence of additional unsprung mass on comfort and safety

The vehicle suspension system may be evaluated in terms of comfort and safety of vehicle users by directly evaluating the vehicle response, determined in the form of variables defined as comfort and safety indicators, to kinematic inputs or by evaluating the characteristics of transforming the kinematic inputs into the said variables (Fig. 2).

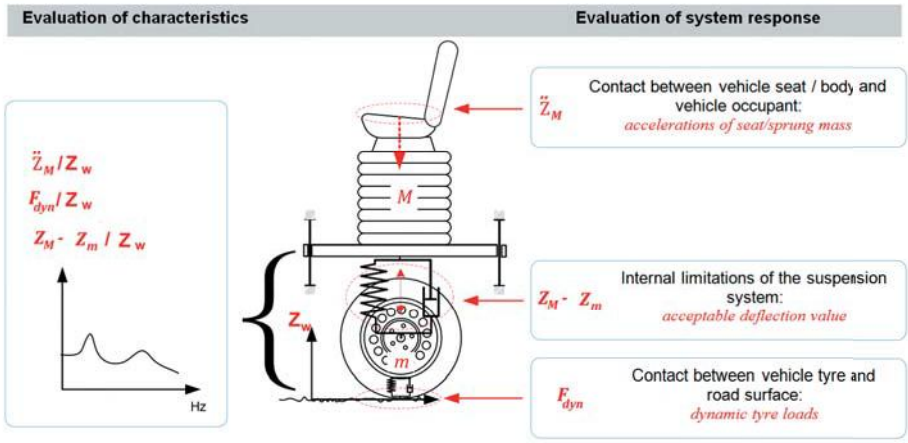

Fig. 2. Vertical vehicle dynamics evaluation methods

In the former case, the evaluation must be carried out for specific inputs (i.e. specific vehicle operation conditions defined by kinematic inputs depending on the type of road surface roughness and the speed of vehicle drive on this road surface), by evaluating the vehicle occupant accelerations as a comfort indicator and dynamic wheel loads as a safety indicator.

In the latter case, the evaluation applies to the way of conversion of kinematic inputs into selected system responses. This evaluation makes it possible to characterize the suspension system regardless of the input applied, with an assumption made that the analysis would be limited to the range where the suspension system operation may be considered linear; for vehicle drives on hard surfaced roads, such an assumption is true within a wide range of vehicle operation conditions.

The latter method of evaluation requires that the input, i.e. the kinematic excitation, should be known. Such an input cannot be measured during an actual vehicle drive; therefore, the analysis of dynamic characteristics cannot be carried out during road tests. However, the dynamic characteristics can be determined experimentally in laboratory conditions, e.g. with the use of electrohydraulic actuators as vibration sources [11].

On the other hand, the analysis of dynamic characteristics can be easily made at model

testing, where both the kinematic input and system response are known. For this reason, this method was employed at the presented simulation analysis of the influence of additional unsprung mass on the vertical dynamics of a motor car.

3. Experimental examination of the influence of additional unsprung mass on the vertical dynamics of a motor car

For the purposes of preliminary exploration of the influence of additional unsprung mass on the vertical dynamics of the car, the torsion-beam rear axle of the test passenger car was modified by adding extra weights to the stub axles.

The influence of additional unsprung mass on the comfort was examined by evaluating, with the use of a standard method, the exposure of a vehicle occupant sitting on a vehicle seat to vertical vibrations (general vibrations) for the test car in its standard version and for the same car with increased unsprung masses and sprung mass. The increase in the sprung mass was represented by loading the car boot with extra weights whose mass was equal to the battery mass. The values of the masses for both cases were as follows, per a single vehicle corner:

1. For the car in its standard version, the unsprung mass was m_2 = 26 kg and the standard sprung mass was m_1 = 207.5 kg;
2. For the car provided with an additional electric powertrain (simulated by extra weights), the unsprung mass was m_2 = 48 kg and the increased sprung mass was m_1 = 230.5 kg.

For the two vehicle configurations as presented above, road tests were carried out, during which vertical accelerations of the sprung mass were measured with the use of sensors placed above the rear axle of the car (Fig. 3a).

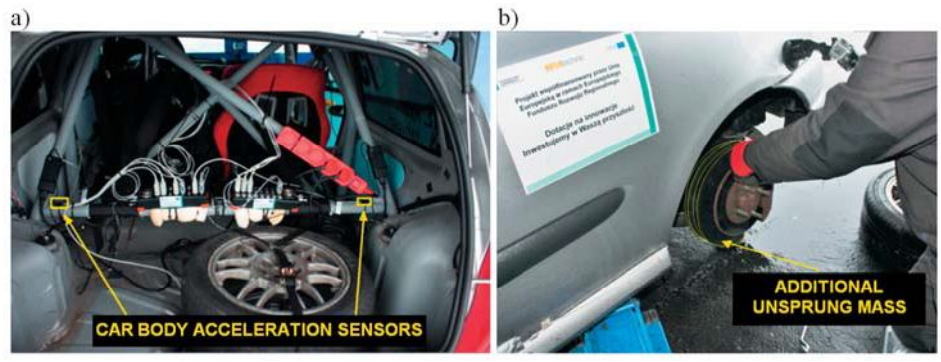

Fig. 3. The test car Renault Clio II: a) Locations of the rear vehicle body part acceleration sensors; b) Location of the weight (non-revolving) that represented the extra unsprung mass

The location of the acceleration sensors was not identical to that required by the method of evaluating the exposure of a vehicle occupant sitting on a vehicle seat to vibrations, where the accelerations should be measured on the appropriate vehicle seat. Such a location was chosen, however, because the tests were aimed at comparing the vertical dynamics of the rear half of the car rather than at direct measurements of the exposure of vehicle occupants to vibrations. This decision was also made because only the unsprung mass of the rear axle was changed and because a simplified model of a rear quarter of the car suspension was used for the computer simulations.

The conditions of the test drives have been specified in Table 1.

Table 1. Road test options chosen

Road surface and vehicle speed	$\mathbf{m_2}$ = 26 kg	$\mathbf{m_2}$ = 48 kg
Asphalt, 60 km/h	X	X
Concrete slabs, 20 km/h	X	X
Crossing of a railway track, 20 km/h	X	X
Crossing of a speed hump, 15 km/h	X	X

The unsprung mass for the standard rear suspension system was determined at laboratory tests; it was 26 kg for a single vehicle corner. To simulate the presence of in-wheel motors, extra weights of 22 kg were added to the unsprung mass for each vehicle corner. A view of the extra weights installed in the car has been presented in Fig. 3b.

The results of measurement of vertical accelerations of the sprung mass were processed in the following stages:

- Filtration of the general vibrations recorded, measured for the car body above the rear axle, in 1/3 octave frequency bands;
- Calculation of RMS vibration acceleration values $\ddot{z}_{M\_RMS}$ [12] in individual 1/3 octave bands;
- Comparison of the obtained distributions of RMS vibration values with the standard limit values for 8 hour time of exposure to vibrations.

Results obtained from the measurement data processing procedure in the form of graphs of RMS values of vertical vibration acceleration $\ddot{z}_{M\_RMS}$ have been presented in Fig. 4.

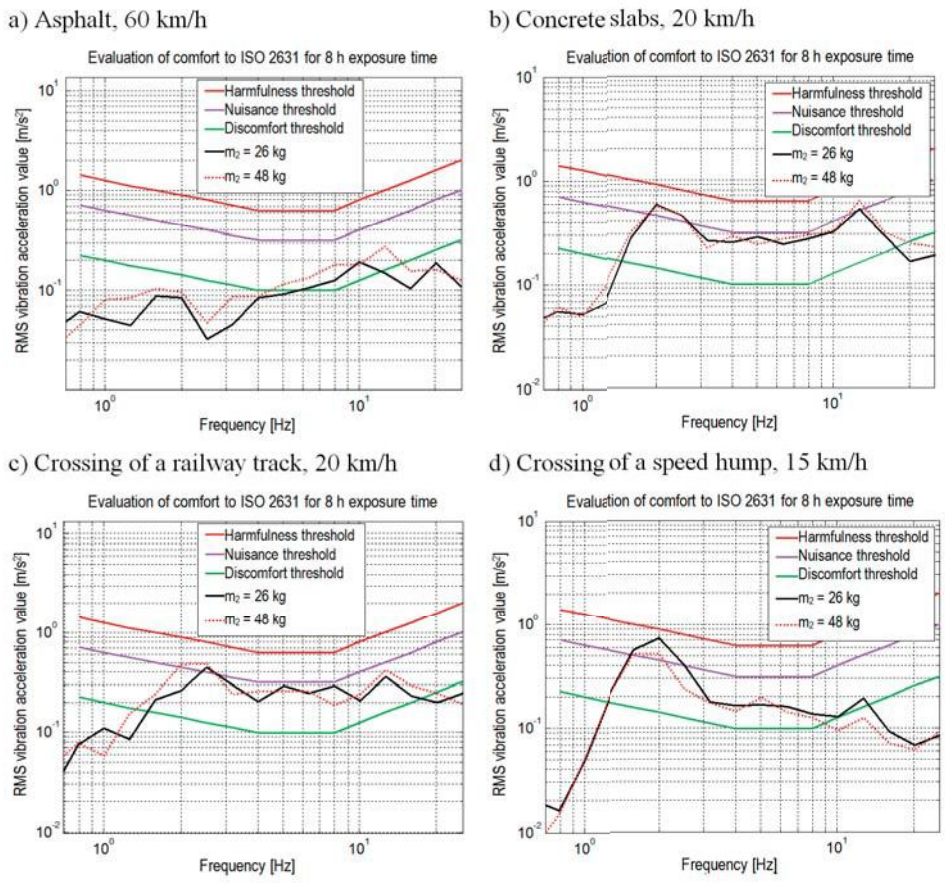

Fig. 4. RMS acceleration values of vertical car body vibrations above the rear axle in 1/3 octave frequency bands from 0.63 Hz to 25 Hz for selected vehicle operation conditions, against the standard limit values according to ISO 2631 for 8 hour time of exposure to vibrations

As regards the results obtained from the analysis of accelerations recorded when the car was driven on an asphalt road, considerable differences chiefly occurred close to the resonance frequency for the unsprung mass m_2. In the 12.5 Hz frequency band, the $\ddot{z}_{M\_RMS}$ value was observed to increase from 0.15 m/s² to 0.28 m/s². For the suspension system with the bigger unsprung mass, the discomfort threshold was exceeded in a wider frequency interval, i.e. from 3.5 Hz to 16 Hz, while this interval for the suspension system with m_2 = 26 kg extended only from 6 Hz to 12.5 Hz. However, this exceedance was quite small and the acceleration values were in both cases considerably lower than the nuisance threshold.

Another big increase, similar to that observed for the frequency band of 12.5 Hz, i.e. by almost 100% again, occurred in the 1.25 Hz frequency band. However, the $\ddot{z}_{M\_RMS}$ values

were in this case much below the discomfort threshold, thanks to which this increase was of no practical importance.

For the test drive on a road made of concrete slabs, the growths recorded were from 0.52 m/s^2 to 0.61 m/s^2 in the 12.5 Hz frequency band and from 0.18 m/s^2 to 0.24 m/s^2 in the frequency band of 20 Hz. In the other frequency bands, the differences were imperceptible. For the railway track crossing, the biggest growth, from 0.25 m/s^2 to 0.48 m/s^2, was recorded in the 2.0 Hz frequency band, which resulted in the nuisance threshold being exceeded in the frequency bands of 2.0 Hz and 2.5 Hz.

An opposite trend was observed when the vehicle crossed the speed hump: in this case, the acceleration values recorded in the 2.0 Hz frequency band were higher by about 50% for the suspension system with lower unsprung mass.

In recapitulation of the description of the experimental tests carried out, a statement may be made that a noticeable impact of the unsprung mass was only observed in the frequency bands covering the resonance frequencies of the sprung and unsprung masses. In the other frequency ranges, this impact was very small. For the car being driven on an asphalt road, which is the most frequent case, the deterioration in the ride comfort was quite small. In most frequency bands, the discomfort threshold was not exceeded and wherever the exceedance occurred the acceleration values were still closer to the discomfort threshold than to the nuisance threshold.

Since the experimental tests only pertained to some selected vehicle operation conditions and could not offer an overall picture of the influence of additional unsprung mass on the ride comfort, a decision was made to carry out simulation research as well.

4. Simulation research on the influence of additional unsprung mass on the vertical dynamics of a motor car

The simulation research was undertaken to estimate theoretically, through evaluation of dynamic characteristics of the car suspension system, the impact of a growth in the mass of the rear vehicle part that would arise from an increase in the unsprung mass of the suspension system and in the sprung mass of the rear part of the car in consequence of the installing of electric motors in vehicle wheels and of the placing of batteries in the car boot, respectively.

4.1. Model of the vertical dynamics of a rear vehicle corner

The vertical dynamics of the quarter-car suspension system was represented by a simplified model with two degrees of freedom, i.e. vertical displacements along the z axis.

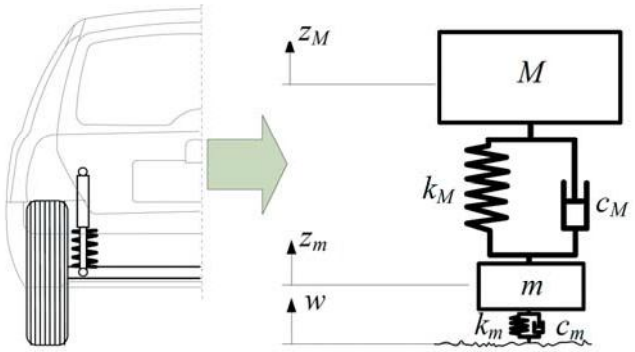

Fig. 5. Sketch showing the simplification of a quarter of the car by reducing it to a model with two degrees of freedom

The model of the vertical dynamics of a motor car suspension system was described by a pair of second-order differential equations of motion:

$$\ddot{z}_M = {}^1\!/_M \cdot (F_{k_M} + F_{c_M}) - g\ ,$$
$$\ddot{z}_m = {}^1\!/_m \cdot [(F_{k_m} + F_{c_m}) - (F_{k_M} + F_{c_M})] - g \tag{1}$$

where: g – acceleration of gravity;

$\ddot{z}_M$ – vertical accelerations of the sprung mass;

$\ddot{z}_m$ – vertical accelerations of the unsprung mass;

F_{k_M}, F_{k_m} – elastic forces of the suspension system and tyre, respectively:

$$F_{k_M} = k_M(z_m - z_M),\ F_{k_m} = k_m(w - z_m) \tag{2}$$

F_{c_M}, F_{c_m} – damping forces of the shock absorber and tyre, respectively:

$$F_{c_M} = c_M(\dot{z}_m - \dot{z}_M),\ F_{c_m} = c_m(\dot{w} - \dot{z}_m) \tag{3}$$

In the model, the F_{k_1} and F_{c_1} force values were interpolated from the shock absorber damping and suspension system stiffness characteristic curves, based on actual suspension deflection $(z_2 - z_1)$ and deflection rate $(\dot{z}_2 - \dot{z}_1)$.

In result of experimental tests carried out, the sprung mass of a rear quarter of the car was found to be as specified in Table 2.

Table 2. Sprung mass of a rear quarter of the car

Car load	Unit	Value
2 occupants, with no wheel weights	kg	207.5
2 occupants + wheel weights + 46 kg in the boot	kg	230.5

Similarly, the unsprung mass for the rear wheels was determined from experimental tests ant its values have been specified in Table 3, depending on the presence of the extra mass.

Table 3. Unsprung mass of a rear quarter of the car

Wheel load	Unit	Value per a single wheel
Without in-wheel motors	kg	26
With in-wheel motors	kg	48

To determine the tyre stiffness, experimental tests were carried out at a tyre inflation pressure of 0.2 MPa. Based on the tests and on an analysis of the test results and in consideration of small nonlinearity of the tyre stiffness curve obtained from the tests, a linear model of the radial tyre stiffness was adopted, with a stiffness coefficient of $\mathbf{k_m}$ **= 175 500 Nm.** For the car in its standard version, loaded with two occupants, the static tyre deflection was 13 mm. For the car with additional unsprung mass and an extra weight in the boot (46 kg), the deflection was 15.6 mm.

The stiffness of the suspension system was also determined experimentally. Based on the experiment results, the stiffness model was assumed as linear, too, with the stiffness coefficient being $\mathbf{k_M}$ **= 36 200 N/m.** The static deflection of the suspension spring for the model adopted was 56.6 mm and the natural frequency was estimated at 2.1 Hz. This stiffness coefficient value is typical for sport suspension systems, such as that provided in the car under tests.

4.2. Simulation of the vehicle response to a sinusoidal input

The mathematical model as described above was implemented in the Matlab-Simulink environment. The model in the graphical form was defined in the Simulink toolbox; the characteristics of suspension system components were defined and a frequency analysis was carried out in the Matlab environment.

To obtain signals for a frequency analysis, according to the objectives of the simulation research carried out, a signal was used that had been prepared as an input for the experimental determining of magnitude-frequency responses at laboratory tests [11] (Fig. 6). This input signal had the nature of a sinusoidal waveform with varying frequency, gradually increasing from 0.1 Hz to 22 Hz, and with amplitude declining from 28 mm to somewhat below 3 mm. The time history of the excitation function applied has been presented in Fig. 6.

When the presented input had been applied and the simulation test had been carried out, time histories of the suspension system response (including sprung mass accelerations $\ddot{z}_M$, tyre deflections $(\dot{w} - \dot{z}_m)$, and dynamic loads F_{dyn}) to the input applied w were recorded.

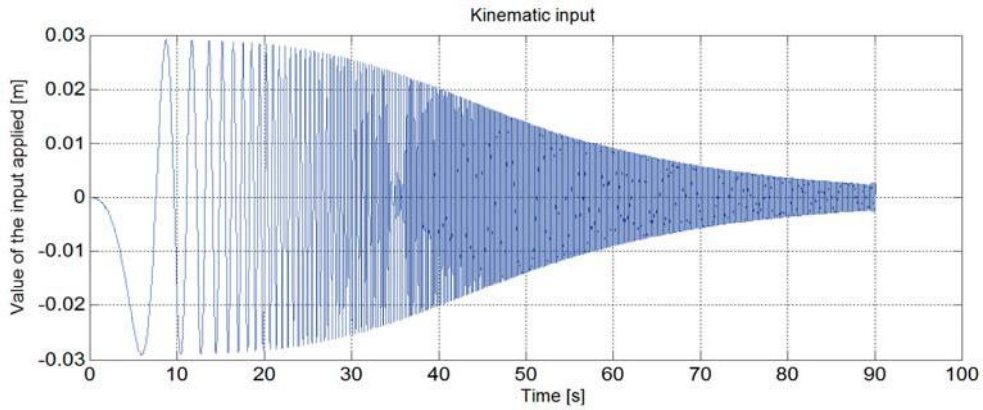

Fig. 6. Kinematic input function used to examine dynamic system characteristics

Two models of a rear quarter of the suspension system of a Renault Clio II car were tested, one of them representing the car in its standard version (with a sprung mass of 207.5 kg and an unsprung mass of 26 kg) and the other one representing the car modified by adding extra weights (with a sprung mass of 230.5 kg and an unsprung mass of 48 kg). In result of the simulation tests carried out, time curves for specific quantities were obtained, which were then analysed in the frequency domain.

4.3. Simulation of the vehicle response to a sinusoidal input

The time histories obtained from the simulation tests were then used for carrying out an analysis in the frequency domain, during which the relation between the excitation and the system responses depending on the excitation frequency was explored. Thanks to appropriate signal processing, "dynamic characteristics" of suspension systems were determined (Fig. 7).

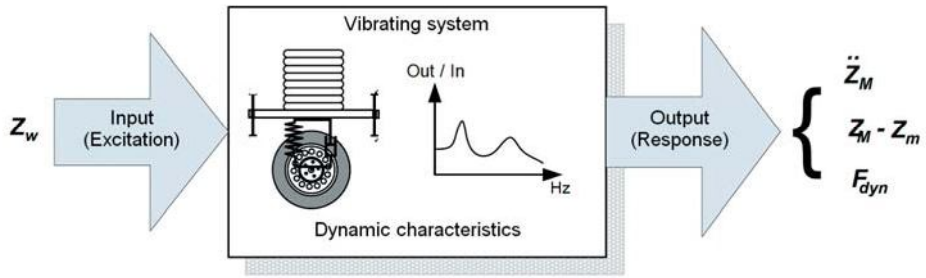

Fig. 7. Quarter-car suspension system as a dynamic system

The knowledge of such characteristics is very important from the point of view of evaluating the quality of suspension system operation in respect of comfort and safety. The comfort is often evaluated through the function of amplification of sprung mass accelerations $\ddot{z}_M(\omega)$; for the evaluation of safety (in terms of maintaining the potential of adhesion forces), the function of amplification of dynamic wheel loads $F_{dyn}(\omega)$ is usually analysed.

To determine frequency characteristics of the suspension system, the signals obtained from the simulation tests were subjected to processing, which was split into the following stages [11]:

- Calculation of an estimate of the transfer function, with making use of estimates of power spectral density and cross-spectral density, according to equation (4):

$$\widehat{H}_{\mathrm{xy}}(\omega) = \frac{\widehat{G}_{\mathrm{xy}}(\omega)}{\widehat{G}_{\mathrm{x}}(\omega)} \tag{4}$$

where: $\widehat{G}_{\mathrm{x}}(\omega)$ – estimator of power spectral density of the input signal;
$\widehat{G}_{\mathrm{xy}}(\omega)$ – estimator of cross-spectral density of the input and output signal.

- Drawing of the modulus and phase of frequency characteristics.

4.4. Results of analysing the dynamic characteristics

The analysis of the influence of changes in the unsprung mass on the comfort was based on analysing the profile of the curve representing the transfer function (i.e. its modulus) for accelerations of the sprung mass (Fig. 8a). This function is interpreted as a function of amplification of the excitation to accelerations $\ddot{z}_M/w$ [9].

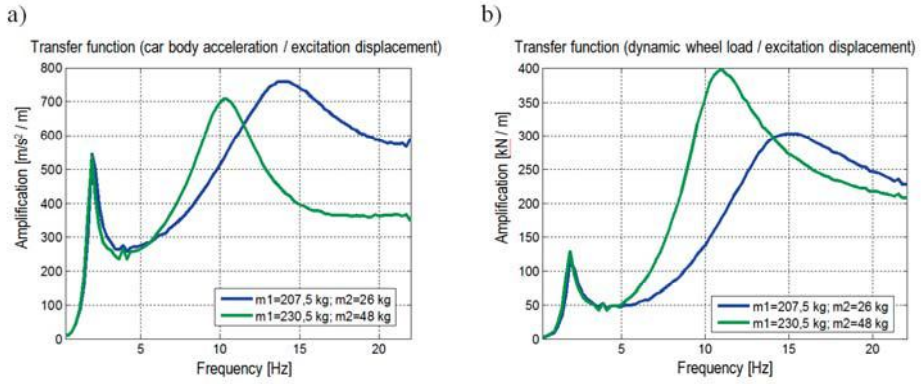

Fig. 8. Selected dynamic characteristics of the suspension system: a) function of amplification of the excitation to accelerations $\ddot{z}_M/w$; b) function of amplification of the excitation to the dynamic wheel load F_{dyn} proportional to tyre deflection $(\dot{w} - \dot{z}_m)/w$

A comparison of values of this function for both suspension system versions, presented in Fig. 8a, has shown that the impact of changes in the unsprung mass on the amplification of accelerations of the sprung mass was of the order of 10%, if merely the maximum values of the amplification function were taken into account. At the system parameters under consideration, the larger unsprung mass in combination with the increased sprung mass brought about a drop in the maximum acceleration values.

If, however, the analysis were carried out for the amplification value as a function of the excitation frequency then it might be noticed that the larger sprung mass resulted in a narrower area of high acceleration amplification values (narrower "resonance" area). For the higher mass value m, moreover, the unsprung mass resonance frequency dropped from about 14 Hz to about 10.5 Hz. The larger unsprung mass also resulted in a significant reduction (by about 30% to 50%) in the acceleration values for frequencies higher than the unsprung mass resonance frequency. Simultaneously, the acceleration values in the area of frequencies below this resonance recorded for the standard vehicle version increased due to a shift of the resonance towards lower frequencies. This means that e.g. in the car operation conditions where the excitation would have a frequency of about 10 Hz, the accelerations would rise by 40%. However, the overall impact on the car ride comfort will depend on the vehicle operation conditions, i.e. spectrum of the road surface roughness and vehicle drive speed, and on the share of specific conditions in the total time of exposure of vehicle occupants to vibrations (an analysis of one specific frequency value is only appropriate when the excitation is stationary).

The analysis of the influence of changes in the unsprung mass on car operation safety was based on analysing the transfer function (i.e. its modulus) for dynamic wheel loads F_{dyn} (Fig. 8b). The values of dynamic wheel loads F_{dyn} should be interpreted as amplitudes of changes in the wheel load in relation to the static wheel load value F_{stat}. Therefore, the higher values of this function, the bigger drop in the instantaneous pressure of the car wheel on the road surface. In an extreme situation, where the product of the amplification and excitation values would become equal to the static wheel load, this would mean a drop in the wheel pressure on the road surface to zero.

When analysing the curve representing the amplification function, one can find that an increase in the unsprung mass resulted in a growth in the extreme values of this function; for the parameters adopted, this growth exceeded 30%. Additionally, this growth may also be observed in the frequency area below the frequency of resonance of the unsprung mass; for frequencies close to the new resonance peak, specific values of the amplification function are higher by even 100% than the corresponding function values for the standard vehicle version. In the area close to the car body resonance frequency, no influence of the additional unsprung mass can be noticed. At frequencies above the wheel resonance, the amplification function values declined by several percent.

For the influence of the additional unsprung mass on the safety of car operation to be analysed, it might be useful to estimate the value of the EUSAMA indicator that is used at diagnostic testing of vehicle suspension systems. Results of such an analysis have been given in Table 4.

Table 4. Analysis of the EUSAMA (EC) indicator for the amplification values obtained

Unsprung mass	Sprung mass	Excitation	Static wheel load	Maximum value of the amplification function	Maximum dynamic wheel load	Minimum wheel load	EUSAMA indicator value
m	M	w	F_{stat}	$Ampl$	F_{dyn}	F_{min}	EC
[kg]	[kg]	[m]	[kN]	[kN/m]	kN	[N]	[%]
26	207.5	0.003	2.29	300	0.9	1.39	60.7
48	230.5	0.003	2.73	400	1.2	1.53	56.0

The increase in the unsprung mass resulted in the EC value being lowered from 60.7% to 56%. In relative terms, this means a decline by about 8% in relation to the value determined for the suspension system with the lower unsprung mass. This impact is lower than it would result from the increase in the unsprung mass taken alone. For the electric drive system being designed, the increase in the unsprung mass is inseparably connected with an increase in the sprung mass and this improves the EUSAMA indicator value because a growth in the sprung mass favourably affects the value of this indicator [10].

The actual values of a drop in the wheel load will depend on current vehicle operation conditions, in particular on road surface roughness and vehicle drive speed. On road sections with the same surface roughness, the wheel-to-road grip may be sooner lost in the case of a suspension system with a higher unsprung mass or this phenomenon will more swiftly occur on a road surface that would be relatively "better", i.e. with lower roughness height.

5. Recapitulation and conclusions

The paper presents results of partial experimental research and simulation tests within the scope of determining the impact of an increase in the unsprung mass with the associated increase in the sprung mass on the comfort and safety of the operation of a motor car. This is inasmuch important as the additional sprung mass reduces to some extent the effect of the additional unsprung mass.

The experimental tests revealed a growth in the RMS vibration acceleration values $\ddot{z}_{M\_RMS}$, especially in the 12.5 Hz frequency band; however, at the typical urban drive speed of the order of 60 km/h, the general level of these accelerations was below, or only slightly exceeded, the discomfort threshold.

The fact that this impact was rather small was confirmed by the simulation analysis carried out. When analysing the maximum values of the amplification function, a statement may even be made that at the system parameters under consideration, the larger unsprung mass brought about a 6% drop in the maximum acceleration values. This is additionally connected with the accompanying increase in the sprung mass, which resulted in an improvement in the comfort [9, 10]. The growths observed in some 1/3 octave frequency

bands were connected with simultaneous shifting of the resonance frequency of the unsprung mass (wheel) towards lower frequencies, i.e. from about 14 Hz to about 10 Hz. In consequence of this shift, the growths or drops in specific frequency ranges were much bigger than changes in the extreme values. Similar results regarding a change in the resonance frequency of the wheel were also presented by the authors of a research work carried out on another front-wheel-drive C segment passenger car, with its unsprung mass being raised by 30 kg [2]. At that work, the resonance frequency of the unsprung mass (wheel) decreased from 14.23 Hz to 9.75 Hz.

An analysis of the estimation of the EUSAMA indicator revealed that, as regards the safety defined by the potential of the adhesion force generated by vertical wheel pressure on the road, the decline in the minimum indicator value was of the order of 8%. This decline may even be reduced by raising the suspension damping ratio.

Conversely, the shift of the resonance frequency towards the lower values must be considered undesirable. As it is for the impact of unsprung mass on the comfort, excitation with a frequency of the order of 10 Hz will result in a significant increase in dynamic wheel loads, even by up to 100% in percentage terms. This translates into a possibility that unfavourable effects of maximum absolute values of dynamic wheel loads, e.g. stability loss at cornering on a rough road surface, may occur when the car is driven with a speed about 25% lower than the speed with which the car with standard unsprung mass could be safely driven on an identical road surface.

References

[1] ADAMS, W.: *Electric Motor*. Patent USA No. 300 827, 1884.

[2] ANDERSON, M.; HARTY, D.: *Unsprung Mass with In-Wheel Motors – Myths and Realities*. 10th International Symposium on Advanced Vehicle Control, Loughborough, UK, 2010.

[3] DONGHYUN, K.; KYEONGHO, S.; YOUNGKWANG, K.; JAESEUNG, C.: *Integrated Design of In-Wheel Motor System on Rear Wheels for Small Electric Vehicle*. World Electric Vehicle Journal Vol. 4, 2010.

[4] HUSAIN, I.: *Electric and hybrid vehicles design fundamentals*. CRC Press LLC, 2003.

[5] Michelin: *Innovation beyond the tire*. http://www.michelin.com/corporate/EN/products/innovation/innovation-beyond-the-tire, visited in May 2013.

[6] SAE: *Siemens VDO drives toward the future*. SAE Technical innovation, 10/2006, http://www.sae.org/ohmag/techinnovations/10-2006/11-14-6-6.pdf, visited in May 2013.

[7] SEIFFERT, R.: *Das Genie und sein Auftrag für eine Technik, die sich nicht durchsetzte. Ferdinand Porsche und der Lohner-Porsche: Mit Frontantrieb und Radnabenmotoren*. Frankfurter Allgemeine Zeitung No. 125, 30 May 2000.

[8] WATTS, A.; VALLANCE, A.; FRASER, A.; WHITEHEAD, A. et al.: *Integrating In-Wheel Motors into Vehicles – Real-World Experiences*. SAE Int. J. Alt. Power, 1(1), pp. 289–307, 2012.

[9] MITSCHKE, M.: *Dynamika samochodu: drgania* (*Motor vehicle dynamics: vibrations*). Vol. 2, WKiŁ, Warszawa 1989.

[10] PIKOSZ, H.; ŚLASKI, G.: *Problem zmienności obciążenia eksploatacyjnego pojazdu w doborze wartości tłumienia w zawieszeniu* (*The problem of vehicle load changes in vehicle suspension damping ratio choice*). Archiwum Motoryzacji, 1/2010.

[11] ŚLASKI, G.: *Experimental determination of suspension magnitude-frequency responses using electro-hydraulic actuators – testing and data processing methods*. The Archive of Automotive Engineering, Vol. 56, No. 2/2012.

[12] WICHER, J.; WIĘCKOWSKI D.: *Influence of vibrations of the child seat on the comfort of child's ride in a car*. Eksploatacja i Niezawodnosc – Maintenance and Reliability, 4(48), 2010.